Medical Engineering and Physics 68 (2019) 11–16

Contents lists available at ScienceDirect

Medical Engineering and Physics

journal homepage: www.elsevier.com/locate/medengphy

Biomechanical comparison of temporomandibular joints after orthognathic surgery before and after design optimization

Jingheng Shu, Yuanli Zhang, Zhan Liu*

Key Lab for Biomechanical Engineering of Sichuan Province, Sichuan University, Chengdu 610065, China

ARTICLE INFO

Article history:
Received 12 October 2018
Revised 22 March 2019
Accepted 31 March 2019

Keywords:
Bilateral sagittal split ramus osteotomy (BSSRO)
Temporomandibular joint (TMJ)
Finite element analysis (FEA)
Stress distribution
Numerical surgery

ABSTRACT

The aim of this study is to analyse the biomechanical effects of bilateral sagittal split ramus osteotomy (BSSRO) on temporomandibular joints (TMJs) of a patient with mandibular prognathism. Two three-dimensional models of the maxilla, mandible, and articular disc were constructed based on pre- and postoperative cone-beam computed tomography (CBCT) images of the patient's head. Meanwhile, based on the preoperative model, numerical surgery of BSSRO was performed to predict the optimized postoperative model (named Num-post). Contact elements were used to simulate the interactions between the discs and articular cartilages and between the upper and lower dentitions. Muscle forces and boundary conditions corresponding to centric occlusion were applied on the models. Stresses on the disc, condylar, and temporal cartilages were significantly reduced after the optimized numerical surgery. Meanwhile, the stress distributions in the TMJ in the Num-post-operative model were uniform without stress concentration compared to Pre-operative model and Post-operative model, which suggests that the optimized numerical surgery can be beneficial to orthognathic surgeries.

1. Introduction

The temporomandibular joints (TMJs) are a pair of complex and highly mobile joints, that undergo more than 2000 movements daily in chewing, biting, swallowing, talking and snoring [1]. The structural and morphological characteristics of TMJs in patients with maxillofacial deformities are anomalous. Mandibular prognathism is a common deformity with a prevalence of 20% [2]. TMJ clicking, pain, disc displacement, disc perforation and osteoarthritis were found in patients with mandibular prognathism [3,4]. Bilateral sagittal split ramus osteotomy (BSSRO) is currently a standard surgery for the correction of mandibular prognathism [5], however, different views on the effects of BSSRO persist [6–8]. Although BSSRO can alter mandibular structures, morphological changes of the TMJ are not considered in the design of orthognathic surgery. Data suggest that BSSRO is beneficial for the functional improvement of the TMJ, in terms of relieving temporomandibular disorders (TMD) [9,10]. In contrast, BSSRO could give rise to the anterior disc displacement, impaired TMJ function and other complications [11–13]. Moreover, reports indicated that the symptoms of TMD were unchanged from the preoperative state after BSSRO [14,15]. From a biomechanical point of view, the location of the mandibular condyle and disc and the internal force of the TMJ can be influenced by BSSRO, thus influencing the postoperative TMJ. Hence, the changes in the stress distribution within TMJs may be a decisive cause for the occurrence of postoperative TMD. That is, orthognathic surgery without consideration of TMJ loads could be a crucial factor leading to complications.

Because of difficulties in the experimental measurement of stress, finite element (FE) analysis is considered as the best way to analyse stress distribution in the TMJ. FE models of the mandible were used to predict the changes of stress in the TMJ implant and evaluate the biomechanical performance of the hybrid technique for fixation [16–18]. Contact elements were introduced to accurately simulate interactions in the TMJ [19,20]. Moreover, the FE models can be used to simulate the mandibular movement. Simulations of jaw opening or lateral excursions were performed to obtain the stress distributions of the disc and retrodiscal tissue [21,22]. The high precision of FE analyses was experimentally validated using 3D printing models, digital speckle pattern interferometry and cadaveric experiments [16,23,24].

The preoperative and postoperative FE models of a patient with mandibular prognathism were used in our study to analyse the stress differences in the TMJ. Furthermore, virtual surgery with biomechanical design was performed to obtain the differences with respect to actual surgery.

* Corresponding author.
E-mail address: bmeliuzhan@163.com (Z. Liu).

https://doi.org/10.1016/j.medengphy.2019.03.018
1350-4533/

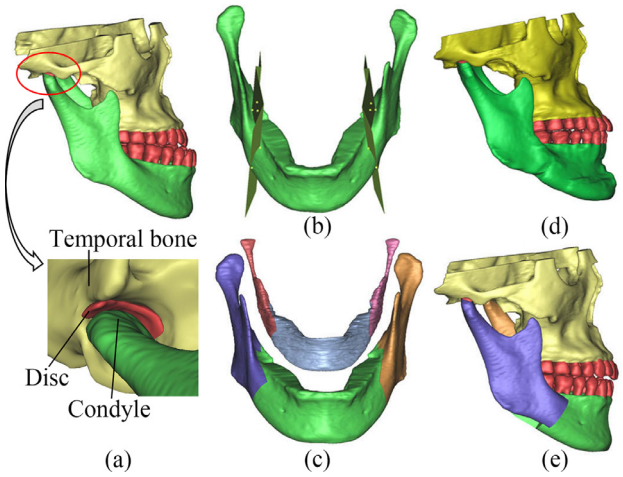

Fig. 1. Numerical surgery process of BSSRO. (a) Pre-operative model and the local region of TMJ; (b) preoperative mandible and osteotomy plane; (c) splitting cancellous and cortical bone; (d) Post-operative model; (e) Num-post-operative model. BSSRO, bilateral sagittal split ramus osteotomy.

Table 1
Material properties of TMJ components.

	Young's modulus (E) (units: MPa)	Poisson's ratio (υ)
Cortical bone [30]	13,700	0.3
Cancellous bone [30]	7930	0.3
Articular cartilage [29]	0.79	0.49
Articular disc [28]	44.1	0.4
Teeth [31]	18,600	0.31

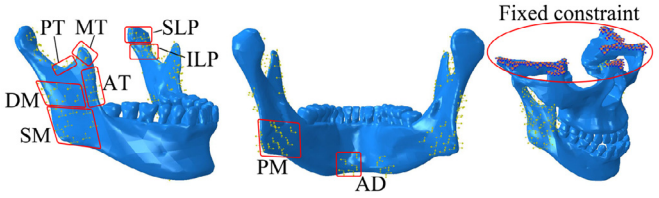

Fig. 2. Loads and boundary constraints of the models. SM, superficial masseter; DM, deep masseter; MP, medial pterygoid; AT, anterior temporalis; MT, middle temporalis; PT, posterior temporalis; ILP, inferior lateral pterygoid; SLP, superior lateral pterygoid; AD, anterior digastric.

2. Materials and methods

2.1. Modelling

2.1.1. Preoperative and postoperative models

The data comprised images from a 24-year-old female patient with mandibular prognathism. The patient underwent BSSRO to retract the mandible at the Affiliated Hospital of Stomatology of Chongqing Medical University. The study was approved by the Institutional Review Board of Chongqing Medical University and the patient provided written informed consent to the use of CT data for the purposes of this study. The patient provided the written informed consent. No signs or symptoms of TMD were found preoperatively, however a clicking joint was detectable at six months post-operative follow-up. The pre- and postoperative (six months post-BSSRO) cone-beam computed tomography (CBCT) scans of the head consisted of 219 images each, with a slice thickness of 0.4 mm. The models including teeth, mandible, and maxilla were reconstructed in MIMICS (Materialise, Leuven, Belgium) based on the levels of grey values. Articular discs were rebuilt in accordance with anatomical characteristics and the shapes of articular surfaces. Subsequently, the models were imported into ABAQUS (ABAQUS. Inc, U.S.A.) and 3D FE models were obtained (Fig. 1(a), (d)). The pre- and postoperative models were named Pre-operative model and Post-operative model, respectively.

2.1.2. Optimized numerical surgery model

Optimized numerical surgery of BSSRO under the guidance of an experienced surgeon was executed on the Pre-operative model in MIMICS. First, three connected incisions on the mandible were performed, i.e. the horizontal, sagittal and vertical osteotomy lines (Fig. 1(b)). Cortical and cancellous bones were completely split by each osteotomy line (Fig. 1(c)). Secondly, the proximal segment and teeth were moved 8 mm backwards and 2 mm upwards, respectively. Meanwhile, the magnitude of the inside rotation was 2° for the right and left mandibular segment. Finally, the overlapped regions of the bilateral mandibular segments were tied together. The mandibular segments were restored at six months post-operation, implying that the mandible healed well without screws in the Num-post-operative model (Fig. 1(e)).

2.1.3. Elements

Cable elements were used to simulate the temporomandibular, sphenomandibular and stylomandibular ligaments [19,25,26]. The condylar and temporal cartilages were modelled as shell elements with a thickness of 0.5 mm [27]. Interactions between the interfaces were considered as contact with a frictional coefficient of 0.001 [19,26]. The modified 10-node quadratic tetrahedron element (C3D10M) and 4-node linear tetrahedron element (C3D4) were used for the contact regions and other structures of the models, respectively. C3D10M elements were used to obtain more accurate results in contact regions, while C3D4 elements were used in other regions to avoid extra calculation time due to more nodes. The 3-node triangular general-purpose shell element (S3) was used for condylar and temporal cartilages. The models were composed of about 100,000 nodes and 210,000 elements.

2.2. Material properties

According to related studies [28–31], the mechanical properties of cortical bone, cancellous bone, articular cartilage, and articular disc were assumed to be homogeneous, isotropic and linearly elastic (Table 1).

2.3. Loading and boundary condition

The loading condition of the central occlusion was applied in the three models. Magnitudes and directions for muscle forces were derived from data available in the literature [32–34]. Nine principal muscle forces were involved in this study (Fig. 2). Each muscle force was evenly distributed on the ten nodes as concentrated force where the load locates, according to the muscle region. The sum of the 10 forces was the same as the corresponding muscle force at the central occlusion. The top surface of the maxilla was fully constrained (Fig. 2).

3. Results

The contact stresses between both the disc and condyle cartilage and the disc and temporal cartilage in the Pre-operative model were greater than those in the Num-post and Post-operative models (Fig. 3). In addition, the maximum contact stress on the disc-condyle cartilage interfaces was higher than that on the disc-temporal cartilage interfaces in the Pre- and Num-post-operative models. However, the opposite trend was found in the Post-operative model.

The tensile and compressive stresses of the disc in the Pre-operative model were much greater than those in the Post- and

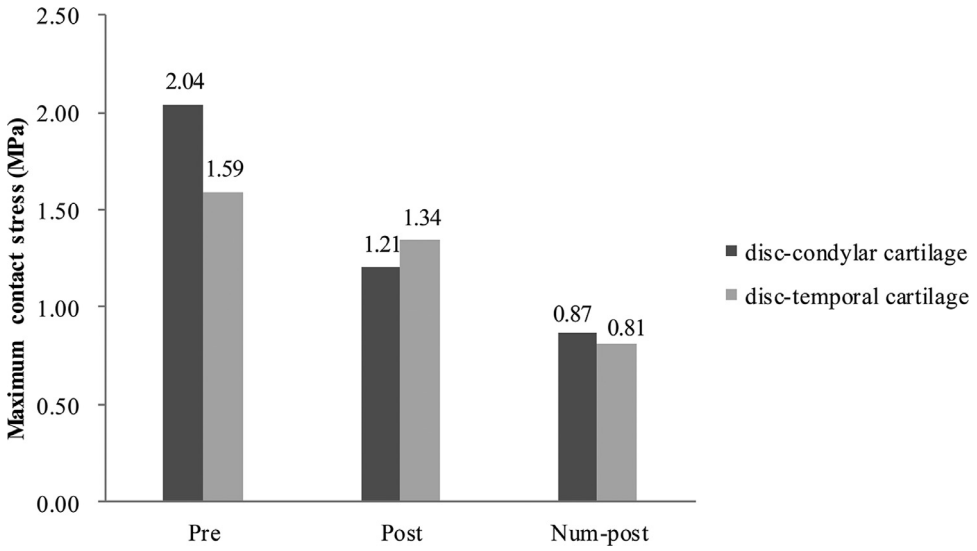

Fig. 3. The maximum contact stresses on the disc-condyle cartilage and disc-temporal cartilage interfaces. Pre, Pre-operative model; Post, Post-operative model; Num-post, Num-post-operative model.

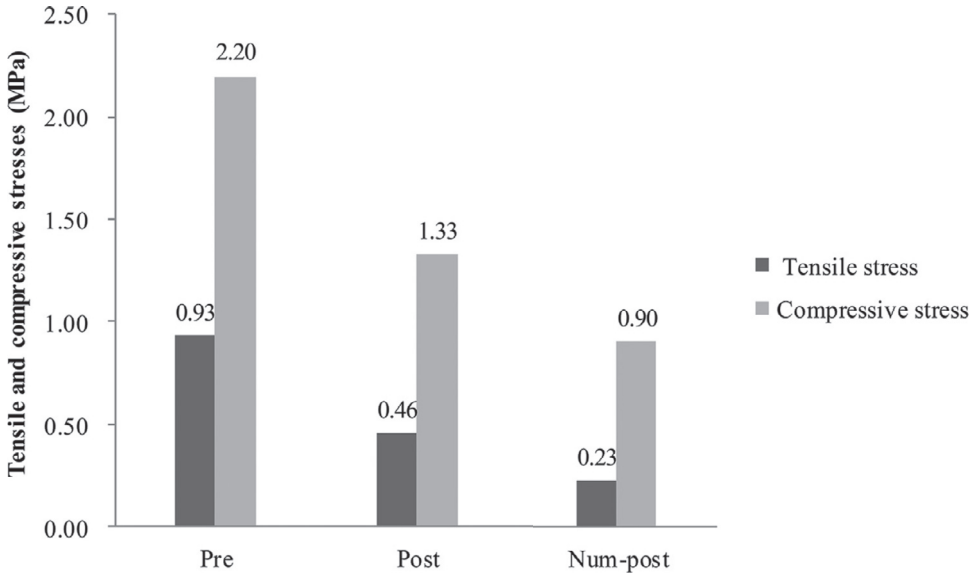

Fig. 4. The maximum tensile and compressive stresses of the disc. Pre, Pre-operative model; Post, Post-operative model; Num-post, Num-post-operative model.

Num-post-operative models (Fig. 4). Moreover, in comparison to the Post-operative model, the Num-post model had lower tensile and compressive stresses.

The maximum von Mises stress of the disc in the Pre-operative model was 1.31 MPa at the posterior band (Fig. 5). The stress concentration nevertheless occurred at the posterior band in the Post-operative model, but the magnitude decreased. In the Num-post-operative model, with the reduction of the stress level, the stress concentration disappeared and the maximum von Mises stress was located at the intermediate zone (Fig. 5).

The von Mises stress of the condylar cartilage was much higher than that of the temporal cartilage in the three models (Fig. 6). Unexpectedly, the maximum von Mises stress of the condylar cartilage in the Post-operative model was located in the anterior region with 242.0 Pa, and it was greater than that of the Pre-operative model. In contrast, the maximum von Mises stress of the condylar cartilage in the Num-post model was located at the anterior region with 113.7 Pa, and it was lower than that of both the Pre- and Post-operative models (Fig. 6). In addition, the maximum von Mises stresses of the temporal cartilage in the Pre-, Post-, and Num-post-operative models were located at the posterior articular eminences, with the magnitude of 20.2, 15.5, and 11.6 Pa, respectively.

4. Discussion

Although BSSRO is usually used to correct jaw deformities, postoperative complications were reported frequently [8,11]. These include postoperative instability, reoperation, and particularly symptoms of TMD [35]. The position and morphology of the TMJ are found to be changed after BSSRO [3,15], however the biomechanical effects of BSSRO for the patients with mandibular prognathism on the TMJ are still of paucity. Meanwhile, the increase of load on the TMJ is considered as one of the main risks of postoperative complications [3,36]. Thus, decreasing the stresses in the TMJ after the surgery is crucial. Therefore, numerical surgery

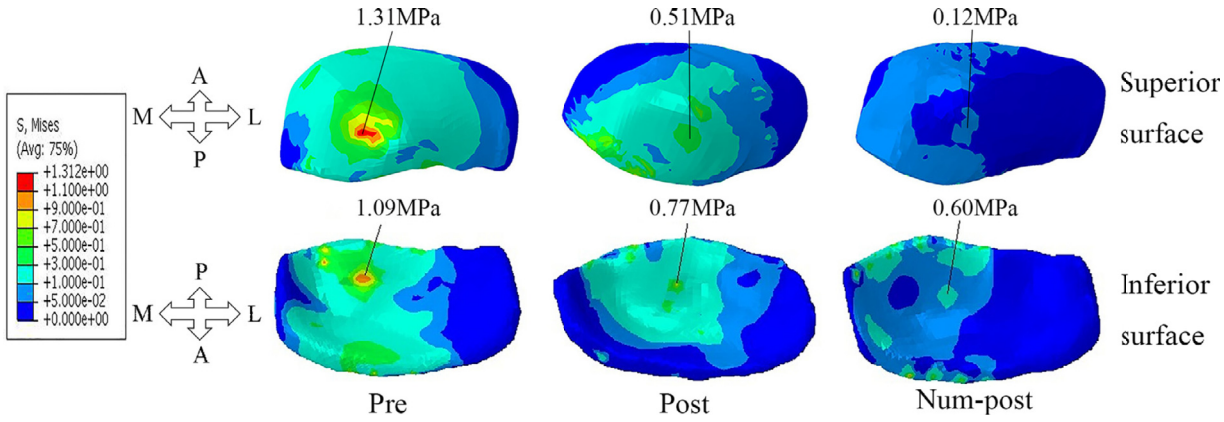

Fig. 5. The von Mises stress distributions of disc in the three models. Pre, Pre-operative model; Post, Post-operative model; Num-post, Num-post-operative model; A, anterior; P, posterior; M, medial; L, lateral.

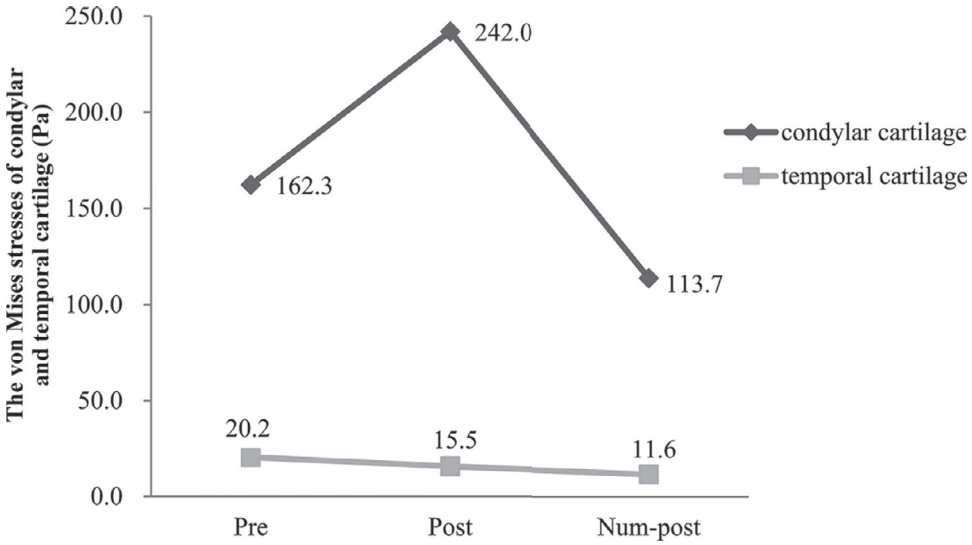

Fig. 6. The maximum von Mises stresses of condyle and temporal cartilages in the three models. Pre, Pre-operative model; Post, Post-operative model; Num-post, Num-post-operative model.

with biomechanical design was introduced in this study, and the stress differences in the TMJ between the actual and virtual surgery were compared. This might be helpful to clinicians for deciding on the strategy of BSSRO.

The interaction on the interfaces between the disc and articular cartilages was considered as frictional contact, which proved to be an effective method to simulate the biomechanics of the TMJ [19,26]. 3D printing model experiments with the pre-defined geometry, material properties, loads, and boundary conditions were performed to validate the precision of FE models [24]. Ten strain rosettes recorded vertical and horizontal strains with the same locations as the FE models. The differences between the experimental and simulated results were less than 5%, which indicates the reliability of the simulations of the TMJ in the current study.

As the anterior teeth of patients with mandibular prognathism cannot bite together, the movements of the TMJ were limited before the surgery. The clinical case reported that occlusion and motion range of the patient improved after the surgery. Moreover, the stresses in the TMJ were improved by BSSRO, but to an extent not comparable with the optimized numerical surgery. The contact stresses of the disc at the two interfaces in the Num-post model were lower than those in the Pre- and Post-operative models. This suggests that the squeezing and extension in the TMJ were reduced after the optimized numerical surgery, and the preoperative pain of the patient was relieved, which is consistent with other studies [37–39]. It is worth mentioning that the contact stresses of the disc-condylar cartilage were lower than those of the disc-temporal cartilage only in the Post-operative model, compared to those in the Pre- and Num-post-operative models. The postoperative clicking may be attributed to the abnormal contact stress distributions at the upper and lower surfaces. Reduction and normalization of the contact stress in the TMJ could recover the normal relationship of the condyle-disc and the temporal bone-disc after the optimized numerical surgery. This could be a factor consider avoiding postoperative clicking.

Furthermore, the high contact stress in the Pre-operative model can lead to excessive tensile and compressive stresses in TMJs. The maximum tensile stress of the disc located at posterior band of the disc in the Pre-operative model, with the magnitude of 0.93 MPa, is close to the tensile failure stress of the posterior band (1.35 MPa) [40]. This high tensile stress in the disc may lead to degenerative changes, such as thinning of the disc, or disc perforation. The decrease of the tensile stresses is beneficial to the postoperative recovery of the TMJ. Meanwhile, the maximum compressive stresses of the disc in the Num-post and Post-operative models were 40.91% and 60.45% of that in the Pre-operative model, respectively. The decreased compressive stress in the Post- and

Num-post-operative models improved the ability to sustain greater pressure, thereby protecting from condylar resorption [41].

The von Mises stresses of the disc in the Post- and Num-post-operative models were also lower than that in the Pre-operative model. However, the maximum von Mises stress was also located at the posterior band of the disc with stress concentration, which is inconsistent with the anatomical structure [42]. The stress distribution of the Num-post model was found to be normal with no stress concentration. Meanwhile, the von Mises stress of the post-condylar cartilage exhibited a significant increase compared to the Pre-operative model, which may result in the postoperative clicking. Therefore, biomechanical predictions should be involved in designing the strategy of BSSRO. Moreover, past orthognathic surgeries did not account for the mechanical environment. In future, it is recommended that virtual surgery is used to predict the postoperative stress distributions following orthognathic surgery. Surgeons could make decisions in the surgical planning according to the simulated results to avoid postoperative TMD.

5. Conclusion

The magnitudes of the stresses in TMJs were reduced and the stress distribution was improved following simulated BSSRO. Moreover, the optimization process predicts postoperative outcomes well, and such numerical models may be used as a tool to provide guidance to surgeons engaged in the treatment of patients with mandibular orthognathism.

Conflict of interest

None.

Funding

This work was supported by the National Natural Science Foundation of China [Grant Nos. 31670963 and 11202143].

Ethical Approval

The protocol of this study was approved by the Affiliated Hospital of Stomatology of Chongqing Medical University Institutional Review Board (CQHS-IRB-2014-01).

References

[1] Mahdian N, Dostalova T, Danek J, Nedoma J, Kohout J, Hubacek M, Hlinakova P. 3D reconstruction of TMJ after resection of the cyst and the stress-strain analyses. Comput Methods Programs Biomed 2013;110:279–89. doi:10.1016/j.cmpb.2012.12.001.

[2] Tang E. The prevalence of malocclusion amongst Hong Kong male dental students. Br J Orthod 1994;21:57–63.

[3] Ueki K, Moroi A, Sotobori M, Ishihara Y, Marukawa K, Yoshizawa K, Kato K, Kawashiri S. Changes in temporomandibular joint and ramus after sagittal split ramus osteotomy in mandibular prognathism patients with and without asymmetry. J Craniofac Surg 2012;40:821–7. doi:10.1016/j.jcms.2012.03.003.

[4] Mikovic N, Lazarevic M, Tatic Z, Krejovic-Trivic S, Petrovic M, Trivic A. Radiographic cephalometry analysis of condylar position after bimaxillary osteotomy in patients with mandibular prognathism. Vojnosanitetski Pregled 2016;73:318–25.

[5] Trauner R, Obwegeser H. The surgical correction of mandibular prognathism and retrognathia with consideration of genioplasty. Part II. Operating methods for microgenia and distoclusion. Oral Surg Oral Med Oral Pathol 1957;10:787–92.

[6] Forssell H, Kauko T, Kotiranta U, Suvinen T. Predictors for future clinically significant pain in patients with temporomandibular disorder: a prospective cohort study. Eur J Pain 2017;21:188–97 (London, England).

[7] Sebastiani AM, Baratto-Filho F, Bonotto D, Kluppel LE, Barbosa RNL, da Costa DJ, Scariotb R. Influence of orthognathic surgery for symptoms of temporomandibular dysfunction. Oral Surg Oral Med Oral Pathol Oral Radiol 2016;121:119–25.

[8] Han JJ, Yang HJ, Lee SJ, Hwang SJ. Relapse after SSRO for mandibular setback movement in relation to the amount of mandibular setback and intraoperative clockwise rotation of the proximal segment. J Craniofac Surg 2014;42:811–15. doi:10.1016/j.jcms.2013.11.018.

[9] Dervis E, Tuncer E. Long-term evaluations of temporomandibular disorders in patients undergoing orthognathic surgery compared with a control group. Oral Surg Oral Med Oral Pathol Oral Radiol Endod 2002;94:554–60. doi:10.1067/moe.2002.128021.

[10] Fang B, Shen GF, Yang C, Wu Y, Feng YM, Mao LX, Xia YH. Changes in condylar and joint disc positions after bilateral sagittal split ramus osteotomy for correction of mandibular prognathism. Int J Oral Maxillofac Surg 2009;38:726–30. doi:10.1016/j.ijom.2009.03.001.

[11] Kim YK, Yun PY, Ahn JY, Kim JW, Kim SG. Changes in the temporomandibular joint disc position after orthognathic surgery. Oral Surg Oral Med Oral Pathol Oral Radiol Endod 2009;108:15–21. doi:10.1016/j.tripleo.2009.02.005.

[12] Okeson JP. Management of temporomandibular disorders and occlusion. 7th ed. USA: Mosby; 2013.

[13] Ueki K, Nakagawa K, Takatsuka S, Yamamoto E. The change of stress distribution on the condyle after mandibular setback surgery. Eur J Orthod 2006;28:433–9. doi:10.1093/ejo/cjl003.

[14] Dicker GJ, Tuijt M, Koolstra JH, Van Schijndel RA, Castelijns JA, Tuinzing DB. Static and dynamic loading of mandibular condyles and their positional changes after bilateral sagittal split advancement osteotomies. Int J Oral Maxillofac Surg 2012;41:1131–6. doi:10.1016/j.ijom.2012.03.013.

[15] Ha MH, Kim YI, Park SB, Kim SS, Son WS. Cone-beam computed tomographic evaluation of the condylar remodeling occurring after mandibular set-back by bilateral sagittal split ramus osteotomy and rigid fixation. Korean J Orthod 2013;43:263–70. doi:10.4041/kjod.2013.43.6.263.

[16] Ramos A, Ballu A, Mesnard M, Talaia P, Simões JA. Numerical and experimental models of the mandible. Exp Mech 2010;51:1053–9. doi:10.1007/s11340-010-9403-x.

[17] Luo D, Rong Q, Chen Q. Finite-element design and optimization of a three-dimensional tetrahedral porous titanium scaffold for the reconstruction of mandibular defects. Med Eng Phys 2017;47:176–83. doi:10.1016/j.medengphy.2017.06.015.

[18] Sato FR, Asprino L, Consani S, Noritomi PY, de Moraes M. A comparative evaluation of the hybrid technique for fixation of the sagittal split ramus osteotomy in mandibular advancement by mechanical, photoelastic, and finite element analysis. Oral Surg Oral Med Oral Pathol Oral Radiol 2012;114:S60–8. doi:10.1016/j.tripleo.2011.08.027.

[19] Liu Z, Fan Y, Qian Y. Comparative evaluation on three-dimensional finite element models of the temporomandibular joint. Clin Biomech (Bristol, Avon) 2008(23 Suppl 1):S53–8. doi:10.1016/j.clinbiomech.2007.12.011.

[20] Chen J, Akyuz U, Xu L, Pidaparti RMV. Stress analysis of the human temporomandibular joint. Med Eng Phys 1998;20:565–72.

[21] Perez Del Palomar A, Doblare M. Finite element analysis of the temporomandibular joint during lateral excursions of the mandible. J Biomech 2006;39:2153–63. doi:10.1016/j.jbiomech.2005.06.020.

[22] Li Q, Ren S, Ge C, Sun H, Lu H, Duan Y, Rong Q. Effect of jaw opening on the stress pattern in a normal human articular disc: finite element analysis based on MRI images. Head Face Med 2014;10:24. doi:10.1186/1746-160X-10-24.

[23] Gröning F, Fagan M, O'Higgins P. Modeling the human mandible under masticatory loads: which input variables are important? Anat Rec Adv Integr Anat Evol Biol 2012;295:853–63. doi:10.1002/ar.22455.

[24] Zhang YL. The effect of bilateral sagittal split ramus osteotomy on temporomandibular joints in patients with facial asymmetry: a morphologic and biomechanical study Ph.D. Thesis. Chengdu: Sichuan University; 2017.

[25] Chen J, Xu LF. A finite element analysis of the human temporomandibular joint. J Biomech Eng 1994;116:401–7.

[26] Liu Z, Fan YB, Qian YL. Biomechanical simulation of the interaction in the temporomandibular joint within dentate mandible: a finite element analysis. In: Proceedings of the IEEE/ICME international conference on complex medical engineering, Beijing; 2007.

[27] Pullinger AG, Baldioceda F, Bibb CA. Relationship of TMJ articular soft tissue to underlying bone in young adult condyles. J Dent Res 1990;69:1512–18.

[28] Tanne K, Tanaka E, M S. The elastic modulus of the temporomandibular joint disc from adult dogs. J Dent Res 1991;70:1545–8.

[29] Woo S, Mow V, Lai W. Biomechanical properties of articular cartilage. Handbook of bioengineering. Skalak R, Chien S, editors. McGraw-Hill; 1987.

[30] Carter D, Hayes W. The compressive behavior of bone as a two-phase porous structure. J Bone Joint Surgery Am Vol 1977;59:954–62.

[31] Tanne K, Koenig HA, CJ B. Moment to force ratios and the center of rotation. Am J Orthod Dentofacial Orthop 1988;94:426–31.

[32] Pruim GJ, de Jongh HJ, ten Bosch JJ. Forces acting on the mandible during bilateral static bite at different bite force levels. J Biomech 1980;13:755–63.

[33] Korioth T, Hannam A. Mandibular forces during simulated tooth clenching. J Orofac Pain 1994;8:178–89.

[34] Weijs WA, Hillen B. Relationship between the physiological cross-section of the human jaw muscles and their cross-sectional area in computer tomograms. Acta Anatomica 1984;118:129–38.

[35] Roh HS, Kim W, Kim YK, JY L. Relationships between disk displacement, joint effusion, and degenerative changes of the TMJ in TMD patients based on MRI findings. J Craniofac Surg 2012;40:283–6.

[36] Shu JH, Yao J, Zhang YL, Chong DYR, Liu Z. The influence of bilateral sagittal split ramus osteotomy on the stress distributions in the temporomandibular joints of the patients with facial asymmetry under symmetric occlusions. Medicine (Baltimore) 2018;97:e11204. doi:10.1097/MD.0000000000011204.

[37] Ueki K, Marukawa K, Shimada M, Hashiba Y, Nakgawa K, Yamamoto E. Condylar and disc positions after sagittal split ramus osteotomy with and without Le Fort I osteotomy. Oral Surg Oral Med Oral Pathol Oral Radiol Endod 2007;103:342–8. doi:10.1016/j.tripleo.2006.05.024.

[38] Namaki S, Maekawa N, Iwata J, Sawada K, Namaki M, Bjornland T, Yonehara Y. Long-term evaluation of swallowing function before and after sagittal split ramus osteotomy. Int J Oral Maxillofac Surg 2014;43:856–61. doi:10.1016/j.ijom.2014.03.001.

[39] Kawakami M, Yamamoto K, Inoue T, Kajihara A, Fujimoto M, Kirita T. Disk position and temporomandibular joint structure associated with mandibular setback in mandibular asymmetry patients. Angle Orthod 2009;79:521–7. doi:10.2319/040708-199.1.

[40] Kang H, Yi XZ, Chen MS. A study of tensile mechanical property of human temporomandibular joint disc. West China J Stomatol 1998;16:253–5.

[41] Arnett GW, Gunson MJ. Risk factors in the initiation of condylar resorption. Semin Orthod 2013;19:81–8. doi:10.1053/j.sodo.2012.11.001.

[42] Beek M, Koolstra JH, van Ruijven LJ, van Eijden TMGJ. Three-dimensional finite element analysis of the human temporomandibular joint disc. J Biomech 2000;33:307–16.